Available online at www.sciencedirect.com

ScienceDirect

Mendeleev Commun., 2022, **32**, 308–310

Mendeleev Communications

Graphene structures prepared *via* pulse alternating current technique

Alexandra B. Kuriganova,*[a] Igor N. Leontyev,[b] Marina V. Avramenko,[b,c] Nikita A. Faddeev[a] and Nina V. Smirnova[a]

[a] *Department of Technology, Platov South-Russian State Polytechnic University, 346428 Novocherkassk, Russian Federation. E-mail: kuriganova_@mail.ru*
[b] *Department of Physics, Southern Federal University, 344006 Rostov-on-Don, Russian Federation*
[c] *Department of Physics, University of Antwerp, 2000 Antwerpen, Belgium*

DOI: 10.1016/j.mencom.2022.05.005

Graphene structures have been obtained by exfoliating thermally expanded graphite using a pulse alternating current technique. The electrochemical properties of these materials used in supercapacitors, lithium-ion batteries and electrocatalysts have been investigated.

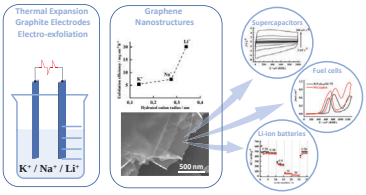

Keywords: graphene, electrochemical exfoliation, pulse alternating current, supercapacitors, Li-ion batteries, fuel cells.

Among various carbon structures such as amorphous carbon, carbon nanotubes, fullerenes and graphene, the latter has unique electrochemical characteristics, making it a promising electrode material for Li-ion batteries (LIBs), supercapacitors (SCs) and electrocatalyst supports.[1–3] At present, methods for producing graphene are represented by mechanical separation of layers from graphite, chemical vapor deposition during the decomposition of hydrocarbons and organic synthesis.[4] Recently, methods based on the electrochemical exfoliation of graphite have attracted increasing interest from researchers due to the possibility of synthesizing graphene structures on a gram scale.[5] Moreover, electrochemical activation of carbon structures, including graphene ones, leads to an improvement in their electrochemical characteristics.[6]

Generally, the electrochemical exfoliation of graphite is carried out under direct potential conditions in aqueous,[7,8] organic[9] or ionic liquid[10,11] electrolytes. However, we have previously shown that pulse alternating current (PAC) conditions intensify the process of dispersion of metal electrodes,[12,13] making it a promising method for the preparation of Pt/graphene[14] and NiO/graphene[15] materials. In this work, we demonstrate the possibility of obtaining graphene structures by the PAC technique in aqueous electrolytes and the prospects for using the obtained graphene as a material for SCs and LIBs, as well as a support for Pt nanoparticles as an electrocatalyst (for details, see Online Supplementary Materials). The mechanism of electrochemical exfoliation of graphite involves the intercalation of anions or cations of electrolytes between graphite layers,[8] and the size and concentration of these ions play a key role in the exfoliation process. Herein, we are trying to determine the influence of the nature of the electrolyte cation on the exfoliation efficiency, *i.e.*, on the dispersion rate of electrodes (V_{disp}) from thermally expanded graphite (TEG).

Determination of the dispersion rate V_{disp} of TEG electrodes in various electrolytes showed that the exfoliation efficiency strongly depends on the hydrated cation radius and increases in the series $K^+ < Na^+ < Li^+$ [Figure 1(*a*)]. At the same time, the I_D/I_G value calculated from the results of Raman spectroscopy shows a different dependence (Figure 1). In the range 1200–3100 cm^{-1} of each Raman spectrum, eight peaks are observed at 1350.5, 1580.5, 1616.7, 2454.3, 2669.4, 2695.8, 2727.9 and 2939 cm^{-1} [Figure 1(*b*)]. The first three peaks can be attributed to the resonance Raman D, G and D′ modes, respectively. The rest, *i.e.*, the G* peak, the complex G′(2D) band and the D+G line, appear due to double-resonance Raman processes. The spectra were fitted with eight Lorentzians [see Figure 1(*b*), green curves], then the I_D/I_G values were calculated as the intensity ratios of the corresponding peaks. Note that defects are understood as defects of both the crystal structure of graphene and its edges. The structure of the G' band is complex: it consists of three peaks located at 2669.4, 2695.8 and 2727.9 cm^{-1}. Although the intensity of this band is much lower than that of the G peak, its shape indicates that the number of graphene layers in the studied sample is more than three.[16,17]

Although in this work we did not explore the effect of the electrolyte on the number of graphene layers, it can be assumed that this number grows with an increase in the rate of

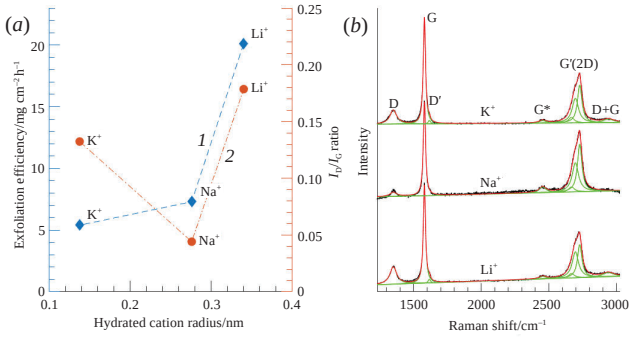

Figure 1 (*a*) Dependences of (*1*) the rate of formation of graphene structures and (*2*) the I_D/I_G value on the radius of the hydrated cation in the electrolyte during electrochemical exfoliation of the TEG electrode using pulse alternating current. (*b*) Fitted Raman spectra of graphene structures obtained in different electrolytes.

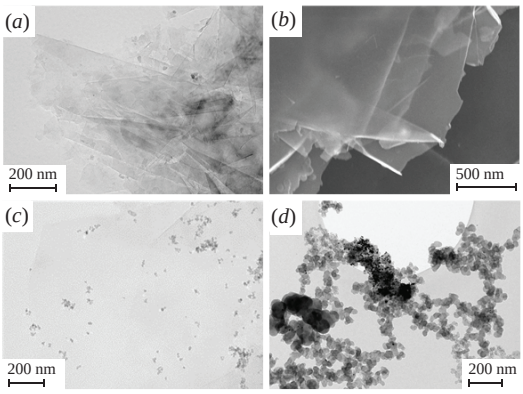

Figure 2 (*a*) TEM and (*b*) SEM images of the graphene structures obtained under PAC conditions. TEM images of (*c*) Pt/graphene and (*d*) Pt/Vulcan XC-72 catalysts, obtained by the PAC technique.

electrochemical exfoliation, which may adversely affect electrochemical characteristics of the material.

Transmission electron microscopy (TEM) and scanning electron microscopy (SEM) data (Figure 2) indicate that thick multilayer graphene flakes with a lateral size of 1–3 μm were formed under PAC conditions in 2 M NaOH solution. Subsequently, due to the optimal value of the exfoliation efficiency, this particular sample was chosen to study its functional properties in various electrochemical applications.

The graphene structures obtained by dispersion of TEG electrodes under the action of pulse alternating current in NaOH electrolyte were studied by cyclic voltammetry in 2 M NaOH electrolyte for use as a supercapacitor material. Cyclic voltammorgams (CVs) of the graphene structures obtained under PAC conditions have a shape typical of carbon materials [Figure 3(*a*)]. It should be noted that there are no quinone–hydroquinone redox peaks, as was previously described[6] for graphene structures after electrochemical activation. The specific capacitance of the graphene structures obtained under PAC conditions was calculated by equation (1) in the potential range from E_1 = 0 mV to E_2 = 1000 mV *vs.* RHE. The specific capacitance weakly depends on the scan rate (v) and amounts to 44–53 F g^{-1} [Figure 3(*b*)].

$$C_S = \int_{E_1}^{E_2} \frac{1}{v} dE \Big/ (E_2 - E_1)m. \quad (1)$$

The intercalation capacity of graphene as an anode material for LIBs is provided by the intercalation/deintercalation of lithium ions between graphene layers and amounts up to 372 mAh g^{-1}. In this case, lithium intercalation proceeds according to the following equation:

$$C_6 + Li^+ + e^- \rightarrow LiC_6. \quad (2)$$

The rate capability of the graphene structures as an active material in LIBs was tested by gradually increasing the cycling rate from C/20 to 2C and then decreasing to C/20. Figure 3(*c*) shows the evolution of the charge and discharge capacity as a function of the cycle number. By reducing the rate from 2C back to C/20, more than 95% of the initial capacity (522 mAh g^{-1}) could be recovered. When cycling the material again at C/20 after the 2C cycling rate, the capacity was 494 mAh g^{-1}. Testing the stability of graphene structures as an active material at C/5 showed a 9.5% decrease in capacity during prolonged cycling [Figure 3(*d*)]. The obtained values of the intercalation capacity of the graphene structures synthesized under the action of a pulse alternating current do not agree with the theoretical model of lithium intercalation into carbon materials and may be associated with the presence of various defects in the anode material[18] and the number of graphene layers.[19]

It is known that graphene structures perform well as supports of Pt nanoparticles and meet all the requirements for supports of electrocatalysts. Previously,[20] we have shown that the reflections in the X-ray diffraction patterns of the Pt/graphene and Pt/Vulcan XC-72 materials correspond only to the face-centered cubic (fcc) structure (space group $Fm\bar{3}m$). The average nanoparticle sizes determined using the Rietveld refinement were 12.73 and 7.04 nm for Pt/Vulcan XC-72 and Pt/graphene, respectively. Figure 3(*e*) displays the CV of the Pt/graphene catalyst in 0.5 M ethanol + 0.5 M H_2SO_4 electrolyte compared to the CV of the Pt/Vulcan XC-72 catalyst with 25% Pt loading, synthesized by a similar method.[21] It should be noted that the currents in the CV curves are normalized to the electrochemically active surface area of platinum, which was determined by the standard CO stripping method. The CVs of both catalysts have an identical form, which indicates that the ethanol oxidation reaction on these catalysts proceeds according to the same mechanism (the Langmuir–Hinshelwood mechanism).[22] Of course, the electrochemical oxidation of ethanol on platinum is a complex multi-stage process, including adsorption, C–C bond cleavage, dehydrogenation, electrooxidation of adsorbed intermediates (*e.g.*, CO and CH_3 species) and the formation of soluble compounds (*e.g.*, acetaldehyde and acetic acid).[23] However, the main stages of the entire process can be described by reactions (3)–(6):

$$Pt + EtOH \rightarrow Pt–CH(OH)Me + H^+ + e^-, \quad (3)$$

$$Pt–CH(OH)Me \rightarrow Pt–CO_{ad} + CH_4 + H^+ + e^-, \quad (4)$$

$$Pt + H_2O \rightarrow Pt–OH_{ad} + H^+ + e^-, \quad (5)$$

$$Pt–CO_{ad} + Pt–OH_{ad} \rightarrow CO_2 + H^+ + e^-. \quad (6)$$

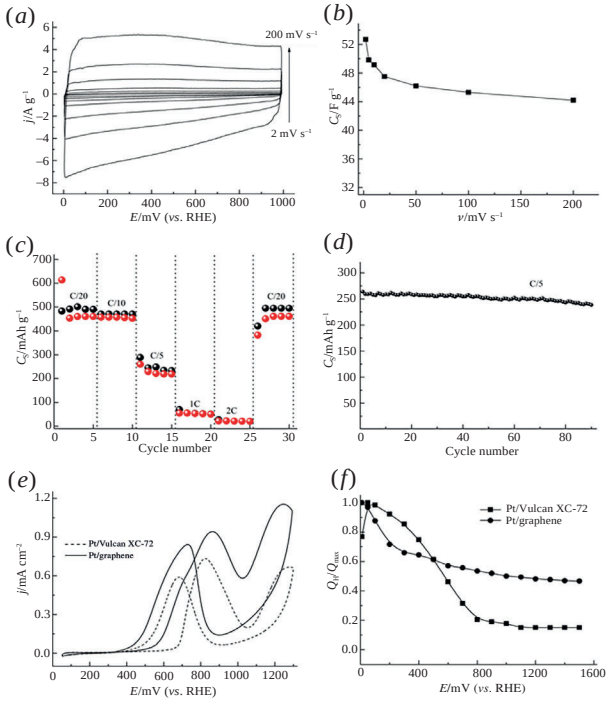

Figure 3 (*a*) CV curves of the graphene structures in 2 M NaOH at a scan rate of 2–200 mV s^{-1}. (*b*) Dependence of the specific capacitance C_s of the graphene structures in 2 M NaOH on the potential scan rate. (*c*) Specific capacitance C_s of the graphene structures as an anode material depending on the cycle number for different C rates in the rate capability experiment (black ball – Q discharge, red ball – Q charge). (*d*) Discharge capacity of the graphene structures as an active material depending on the cycle number in the long-term cyclability test. (*e*) CV curves of the graphene structures and Vulcan XC-72 carbon black decorated with Pt nanoparticles in 0.5 M ethanol + 0.5 M H_2SO_4 electrolyte at a scan rate of 20 mV s^{-1}. (*f*) Stability test of the graphene structures and Vulcan XC-72 carbon black decorated with Pt nanoparticles in 0.5 M H_2SO_4 electrolyte.

As can be seen in Figure 3(*e*), for the Pt/graphene catalyst, the ethanol oxidation rate is higher and the ethanol overpotential (onset potential) is lower than for the Pt/Vulcan XC-72 catalyst, which may be due to the lower degree of agglomeration of Pt nanoparticles on the surface of the graphene structures compared to Vulcan XC-72 carbon black [see Figure 2(*c*),(*d*)]. In addition, the stability during prolonged cycling was higher for the graphene-based electrocatalyst than for the Vulcan XC-72 carbon black catalyst [Figure 3(*f*)].

The obtained results of studying the efficiency of the graphene structures synthesized using the PAC technique are comparable with the results of other studies of pure graphene as an electrode material for a supercapacitor and a lithium-ion battery, as well as a support for Pt nanoparticles in an electrocatalyst (Table S1, see Online Supplementary Materials).

In summary, we have shown that the pulse alternating current technique, which was previously used to obtain nanoparticles of metals and metal oxides, is also applicable to the production of graphene structures. We have established that the exfoliation efficiency depends on the nature of the electrolyte cation, and the formation rate of graphene structures decreases with increasing radius of the hydrated cation. We have demonstrated that the resulting graphene structures are promising for use both as an active material for supercapacitors and lithium-ion batteries, and as a support for Pt-containing catalysts in fuel cells. It can be assumed that further optimization of the electrochemical synthesis conditions, such as the nature of the electrolyte anion and alternating current parameters, will make it possible to obtain graphene structures with adjustable properties, such as the number of layers and lateral dimensions, which will have a positive effect on the use of such materials in relevant applications.

This work was supported by the Ministry of Science and Higher Education of the Russian Federation within the framework of the State assignment in the field of fundamental research under the project ‘Hydrogen fuel cells for small unmanned aerial vehicles: modeling, development, research’ (scientific code FENN-2020-0020).

Online Supplementary Materials

Supplementary data associated with this article can be found in the online version at doi: 10.1016/j.mencom.2022.05.005.

References

1 S. Hossain, A. M. Abdalla, S. B. H. Suhaili, I. Kamal, S. P. S. Shaikh, M. K. Dawood and A. K. Azad, *Journal of Energy Storage*, 2020, **29**, 101386.
2 A. G. Olabi, M. A. Abdelkareem, T. Wilberforce and E. T. Sayed, *Renewable Sustainable Energy Rev.*, 2021, **135**, 110026.
3 R. V. Borisov, O. V. Belousov, A. M. Zhizhaev, M. N. Likhatski and N. V. Belousova, *Russ. Chem. Bull.*, 2021, **70**, 1474.
4 V. B. Mohan, K.-t. Lau, D. Hui and D. Bhattacharyya, *Composites, Part B*, 2018, **142**, 200.
5 S. K. Sahoo, A. K. Behera, R. Chandran and A. Mallik, *J. Appl. Electrochem.*, 2020, **50**, 673.
6 V. A. Krivchenko, Y. M. Maksimov, B. I. Podlovchenko, A. T. Rakhimov, N. V. Suetin and M. A. Timofeev, *Mendeleev Commun.*, 2011, **21**, 264.
7 A. Ambrosi and M. Pumera, *Chem. – Eur. J.*, 2016, **22**, 153.
8 P. Yu, S. E. Lowe, G. P. Simon and Y. L. Zhong, *Curr. Opin. Colloid Interface Sci.*, 2015, **20**, 329.
9 M. H. Chakrabarti, N. S. A. Manan, N. P. Brandon, R. C. Maher, F. S. Mjalli, I. M. AlNashef, S. A. Hajimolana, M. A. Hashim, M. A. Hussain and D. Nir, *Chem. Eng. J.*, 2015, **274**, 213.
10 H. Yang, C. Shan, F. Li, D. Han, Q. Zhang and L. Niu, *Chem. Commun.*, 2009, 3880.
11 N. Liu, F. Luo, H. Wu, Y. Liu, C. Zhang and J. Chen, *Adv. Funct. Mater.*, 2008, **18**, 1518.
12 A. B. Kuriganova, I. N. Leontyev, A. S. Alexandrin, O. A. Maslova, A. I. Rakhmatullin and N. V. Smirnova, *Mendeleev Commun.*, 2017, **27**, 67.
13 A. A. Ulyankina, A. B. Kuriganova and N. V. Smirnova, *Mendeleev Commun.*, 2019, **29**, 215.
14 A. B. Kuriganova, I. N. Leontyev, M. V. Avramenko, Y. Popov, O. A. Maslova, O. Yu. Koval and N. V. Smirnova, *ChemistrySelect*, 2017, **2**, 6979.
15 D. V. Chernysheva, I. N. Leontyev, M. V. Avramenko, N. V. Lyanguzov, T. I. Grebenyuk and N. V. Smirnova, *Mendeleev Commun.*, 2021, **31**, 160.
16 A. C. Ferrari, J. C. Meyer, V. Scardaci, C. Casiraghi, M. Lazzeri, F. Mauri, S. Piscanec, D. Jiang, K. S. Novoselov, S. Roth and A. K. Geim, *Phys. Rev. Lett.*, 2006, **97**, 187401.
17 Y. Hernandez, V. Nicolosi, M. Lotya, F. M. Blighe, Z. Sun, S. De, I. T. McGovern, B. Holland, M. Byrne, Y. K. Gun’Ko, J. J. Boland, P. Niraj, G. Duesberg, S. Krishnamurthy, R. Goodhue, J. Hutchison, V. Scardaci, A. C. Ferrari and J. N. Coleman, *Nat. Nanotechnol.*, 2008, **3**, 563.
18 D. Datta, J. Li, N. Koratkar and V. B. Shenoy, *Carbon*, 2014, **80**, 305.
19 X. Tong, H. Wang, G. Wang, L. Wan, Z. Ren, J. Bai and J. Bai, *J. Solid State Chem.*, 2011, **184**, 982.
20 A. B. Kuriganova, I. N. Leontyev, O. A. Maslova and N. V. Smirnova, *Mendeleev Commun.*, 2018, **28**, 444.
21 I. Leontyev, A. Kuriganova, Y. Kudryavtsev, B. Dkhil and N. Smirnova, *Appl. Catal., A*, 2012, **431**–**432**, 120.
22 J. Flórez-Montaño, G. García, O. Guillén-Villafuerte, J. L. Rodríguez, G. A. Planes and E. Pastor, *Electrochim. Acta*, 2016, **209**, 121.
23 R. Rizo, S. Pérez-Rodríguez and G. García, *ChemElectroChem*, 2019, **6**, 4725.

Received: 11th October 2021; Com. 21/6721